(6) Decker, C. *Polym. Prepr. (Am. Chem. Soc., Div. Polym. Chem.)* **1984**, *25*, 303.
(7) Decker, C. *ACS Symp. Ser.* **1984**, *No. 266*, 207.
(8) Decker, C. *Polym. Mater. Sci. Eng.* **1983**, *49*, 32.
(9) Decker, C.; Moussa, K. *Polym. Mater. Sci. Eng.* **1986**, *55*, 552.
(10) Decker, C. *Radiation Curing of Polymers*; Randell, D. R., Ed., Society of Chemistry: London, 1987; Vol. 64, p 16.
(11) Decker, C. *Polym. Photochem.* **1983**, *3*, 131.
(12) Decker, C.; Jenkins, A. *Macromolecules* **1985**, *18*, 1241.
(13) Decker, C. *Radcure Proceedings* FC 83-265, 1983.
(14) Olaj, O. F.; Bitai, I.; Kauffmann, H. F.; Gleixner, G. *Oesterr. Chem. Z.* **1983**, *84*, 264.
(15) Olaj, O.; Bitai, I.; Gleixner, G. *Makromol. Chem.* **1985**, *186*, 2569.
(16) Olaj, O.; Bitai, I.; Hinkelmann, F. *Makromol. Chem.* **1987**, *188*, 1689.
(17) Olaj, O.; Bitai, I. *Angew. Makromol. Chem.* **1987**, *155*, 177.
(18) Olaj, O.; Bitai, I. *Makromol. Chem. Rapid Commun.* **1988**, *9*, 275.
(19)
(20) Fouassier, J. P.; Lougnot, D. J.; Pilot, T. *J. Polym. Sci., Polym. Chem. Ed.* **1985**, *23*, 569.
(21) Fouassier, J. P.; Lougnot, D. J. *Makromol. Chem.* **1983**, *4*, 11.
(22) Williamson, M. A.; Smith, J. D. B.; Castle, P. M.; Kauffman, R. N. *J. Polym. Sci., Polym. Chem. Ed.* **1982**, *20*, 1875.
(23) Sadhir, R. K.; Smith, J. D. B.; Castle, P. M., *J. Polym. Sci., Polym. Chem. Ed.* **1983**, *21*, 1315.
(24) Sadhir, R. K.; Smith, J. D. B.; Castle, P. M., *J. Polym. Sci., Polym. Chem. Ed.* **1985**, *23*, 411.
(25) Hoyle, C. E.; Hensel, R. D.; Grubb, M. B. *J. Polym. Sci., Polym. Chem. Ed.* **1984**, *22*, 1865.
(26) Hoyle, C. E.; Hensel, R. D.; Grubb, M. B. *J. Radiat. Curing* **1984**, *11*(4), 22.
(27) Hoyle, C. E.; Hensel, R. D.; Grubb, M. B. *Polym. Photochem.* **1984**, *4*, 69.
(28) Hoyle, C. E.; Trapp, M. A.; Chang, C. H. *Polym. Mater. Sci. Eng.* **1987**, *57*, 579.
(29) Hoyle, C. E.; Chawla, C. P.; Chatterton, P. M.; Trapp, M. A.; Chang, C. H.; Griffin, A. C. *Polym. Prepr. (Am. Chem. Soc., Div. Polym. Chem.* **1988**, *29*(1), 518.
(30) Hoyle, C. E.; Trapp, M. A.; Chang, C. H.; Latham, D. D.; McLaughlin, K. W. *Macromolecules* **1989**, *22*, 35.
(31) Hoyle, C. E.; Trapp, M. A.; Chang, C. H., *J. Polym. Sci., Part A Polym. Chem.*, in press.
(32) Hoyle, C. E.; Trapp, M. A.; Chang, C. H.; Latham, D. D.; McLaughlin, K. W., submitted for publication in *Macromolecules*.
(33) Latham, D. D.; McLaughlin, K. W.; Hoyle, C. E.; Trapp, M. A. *Polym. Prepr. (Am. Chem. Soc., Div. Polym. Chem.)* **1988**, *29*(2), 328.
(34) McLaughlin, K. W.; Latham, D. D.; Hoyle, C. E.; Trapp, M. A., submitted for publication in *J. Phys. Chem.*
(35) Chin, S. L. *Can. J. Chem.* **1976**, *54*, 2341.
(36) Oraevskii, A. N.; Pimenov, V. P.; Stepanov, A. A.; Shcheglov, V. A. *Sov. J. Quantum Electron. (Engl. Transl.)* **1974**, *4*(5), 711.
(37) Aleksandrov, A. P.; Genkin, V. N.; Kital, M. S.; Smirnova, I. M.; Sokolov, V. V. *Sov. J. Quantum Electron. (Engl. Transl.)* **1977**, *7*(5), 547.
(38) Hatchard, C. G.; Parker, C. A. *Proc. R. Soc. London, A* **1956**, *235*(A), 518.
(39) Calvert, J. G.; Pitts, J. N. *Photochemistry*; Wiley: 1966; pp 780–786.
(40) North, A. M. *Reactivity, Mechanism and Structure in Polymer Chemistry*; Wiley-Interscience: New York, 1974; Chapter 5, p 142.
(41) O'Driscoll, K. F.; Mahabadi, H. K. *J. Polym. Sci., Polym. Chem. Ed.* **1976**, *14*, 869.
(42) O'Driscoll, K. F.; Davis, T. P.; Piton, M. C.; Winnik, M. A. *J. Polym. Sci., Polym. Lett.* **1989**, *27*, 181.

Uniting Molecular Network Theory and Reptation Theory To Predict the Rheological Behavior of Entangled Linear Polymers

Bernard J. Meister

Designed Thermoplastics Research, The Dow Chemical Company, Midland, Michigan 48667. *Received November 2, 1988; Revised Manuscript Received February 27, 1989*

ABSTRACT: A new model is presented for the description of the linear viscoelastic behavior of entangled linear polymer chains. The equations are derived by combining the structure of molecular network theory, the concept of forced segmental reptation around entanglement junctions, and the reptation description of path length. The resulting equations for monodisperse melts show crossover with the Rouse equation at $M/M_e = 3.21$ and crossover with a modified tube diffusion result at $M/M_e = 380$. Over two decades of molecular weight, a result close to $\eta_0 \sim M^{3.4}$ is obtained. The equations also predict a value of $J_e^0G^0$ of 2.462 for monodisperse melts. An explicit equation for the viscosity of binary blends is obtained, which agrees well with the empirical rule $\eta_0 \sim M_w^{3.5}$. Further comparisons to the steady shear compliance J_{e_b} and loss modulus data for binary blends of polybutadiene demonstrate good predictive ability of the complete relaxation spectrum. As this theory describes molecular motions that are imposed by the deformation, it is consistent with self-diffusion data showing $D \sim M^{-2}$. The quantitative agreement of the two constants with accepted values lends considerable support that the modes of motion described are a realistic description of the molecular dynamics.

Introduction

The effect of molecular weight and molecular weight distribution on the chain dynamics of entangled linear polymer chains has been a subject of intense interest for 30 years. Since the early Graessley theories,[1,2] many approaches have been tried to describe the observed behavior. It has been well established experimentally that the zero-shear viscosity η_0 can be well correlated with the weight-average molecular weight $\bar{M}_w$ by the expression

$$\eta_0 = K\bar{M}_w^{\alpha} \quad (1)$$

where α varies only slightly from polymer to polymer from 3.3 to 3.6.[3,4] This is generally true for all molecular weights above a critical molecular weight, M_c, where M_c is approximately $2M_e$ and M_e is the molecular weight between entanglements as defined by the shear modulus G^0

$$G^0 = \rho RT/M_e \quad (2)$$

where ρ is the polymer concentration, R is the universal gas constant, and T is the temperature. Both the shear modulus G^0 and the steady-state compliance J_e^0 are independent of molecular weight for monodisperse systems above M_c and the product $J_e^0G^0$, which is a measure of the breadth of the spectrum of chain motions, is generally

0024-9297/89/2222-3611$01.50/0

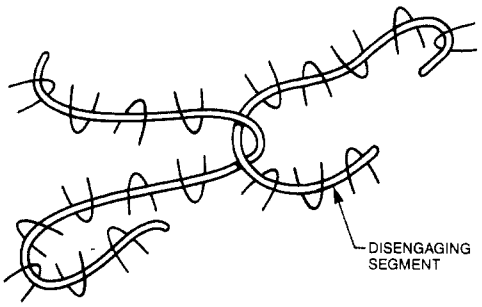

Figure 1. Representation of an entanglement within matrix constraints.

around 2.50. The steady-state compliance shows strong effects of polydispersity and is often a critical test for theories of molecular weight distribution on chain dynamics. The value of J_e^0 increases rapidly with addition of a small number of long chains to a short-chain matrix[5-7] with a maximum at approximately

$$\phi_L = M_S/2.0M_L \tag{3}$$

where M_S and M_L are the molecular weights of the short and long chains, respectively, and ϕ_L is the volume or weight fraction of the long chains in the mixture.

The concept of reptation, first proposed by de Gennes[8] as the primary mode of polymer chain dynamics, has renewed interest in molecular-based descriptions. Notable successes are the description of monodisperse diffusion data and qualitative predictions of Doi–Edwards tube model,[9] which extends the reptation concept to a general constitutive equation. Notable failures have been the prediction that α in eq 1 is 3.0 and most polydispersity effects.

Recent data on self-diffusion in polydisperse systems[10] have shown clearly that the diffusion of long chains is substantially accelerated in a short-chain matrix. Recently introduced concepts of constraint release and tube renewal[11-14] have been introduced into the tube model equations to obtain better predictions for polydisperse systems. Although they accomplish this end, none of these approaches solves the problem of $\alpha = 3.0$. It has been suggested[15] that chain-end fluctuations can be the cause of higher values of α, but quantitative agreement is not good.[16] For further background, see a recent review.[17]

The general conclusions one can make from the foregoing discussion is that monodisperse linear polymers of molecular weight greater than M_c relax stresses by moving along a primary path that has a length scale that is proportional to molecular weight and this path length is strongly affected when this chain is placed in a low molecular weight matrix. In this paper, rather than focus on chains relaxing through tubes, attention will be focused on the entanglement junctions as is done in molecular network theory, and the reptational modes required to relax the stresses at the junctions will be analyzed.

The Monodisperse Case

Consider an entanglement junction between two chains as shown in Figure 1. Both chains are involved in many other entanglements, the number of which can be designated as M/M_e where M_e is the molecular weight between entanglements. It is, of course, these restrictive entanglements that cause the primitive path of the molecular motion to be proportional to molecular weight. When the material is placed under stress, one possible mode of relaxation is for one of the molecules to reptate around the entanglement junction. The energy E_i dissipated by this motion is given by

$$E_i = \xi_0 L_i P_i V_i \tag{4}$$

where ξ_0 is the monomeric friction coefficient, L_i is the number of monomer units in the disengaging segment, P_i is the length of the path it follows, and V_i is the relative velocity at which the segment moves through the matrix.

Since the viscosity η is just the energy dissipated per unit volume divided by the shear rate γ, we arrive at

$$\eta = \sum_i \frac{N_i \xi_0 L_i P_i V_i}{\dot{\gamma}} \tag{5}$$

where N_i is the number of entanglements per unit volume of disengaging length L_i. The length of the segment is simply

$$L_i = m_i/M_0 \tag{6}$$

To use the normal definition of the monomeric friction coefficient, m_i is the molecular weight of the segment and M_0 is the monomeric molecular weight.

It is reasonable to assume, as did Graessley[2] that the disengaging segment will be the smallest of the four that are involved in the entanglement, as this will minimize energy dissipation.

It is assumed by eq 6 that all the extra relative velocity required to disengage the segment from the entanglement locus is taken on by the disengaging segment and that the rest of the molecule moves along at an average velocity equal to the locus of its center of gravity. This is a primary distinction between what we here call "forced reptation" and normal diffusional reptation, which involves the whole molecule. It will later be shown that there is a molecular weight above which less energy is dissipated by diffusion of the whole molecule through its tube than by forced segmental reptation but that this molecular weight is higher than most experimental data.

If we treat the entanglement density ν as a constant independent of molecular weight and let random statistics apply to the entanglements, then the distribution of shortest segments will be

$$N_i = \frac{4.0\phi^2\nu(M - 2m_i)}{M^2} \tag{7}$$

where the total number of junctions is given by

$$N_t = \int_0^{M/2} N_i \, dm_i = \phi^2\nu \tag{8}$$

ν is defined by

$$\nu = G^0/kT = \rho N/M_e \tag{9}$$

and N is Avogadro's number.

To determine path length, the simplest concept is to treat the chain segment m_i as a necklace of beads where each bead is a random chain of length m_i/N_e and N_e is the number of effective constraints. Each bead has diameter $2a\,(m_i/N_e)^{1/2}$. The parameter a is defined by the mean-square end-to-end distance of a chain segment of length M_e of the polymer in question.

The analysis to determine the number of constraining entanglements is the same as done at the main junction. At each junction, one only considers whether the disengaging segment is longer than the shortest part of the crossing molecule. If the crossing molecule has the shorter segment, then it does not serve as a constraint to the path of the disengaging segment. Therefore, constraint release becomes a natural part of the overall theory.

If the segment is less than $M/2$ in length, which is always true in the monodisperse case, then the number of effective entanglements N_e is just the number of entanglements per

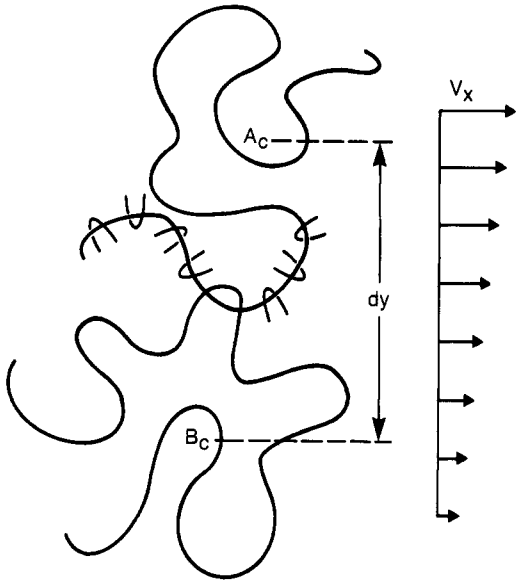

Figure 2. Illustration of an entanglement junction being pulled apart in a velocity gradient.

disengaging segment multiplied by the probability the crossing molecule is an effective constraint

$$N_e = \frac{m_i}{M_e}(1.0 - m_i/M) \tag{10}$$

and the total effective path length P_m is

$$P_m = 2a(m_i/N_e)^{1/2}N_e = \frac{2am_i}{M_e^{1/2}}[1.0 - (m_i/M)]^{1/2} \tag{11}$$

and the average path for monomeric units within segment m_i for insertion in eq 4 will be

$$P_i = \frac{am_i[1.0 - (m_i/M)]^{1/2}}{M_e^{1/2}} \tag{12}$$

The velocity term in eq 4 is the term that brings the most distinction from the well-known tube model result. The velocity can be written as

$$V_i = P_m/t_d \tag{13}$$

where P_m is the path length of the end of the segment defined by eq 11 and t_d is the time for the disengaging segment to clear the junction. It should be clear that it is the imposed macroscopic deformation that is causing the forced reptation. The situation is as shown in Figure 2.

Molecule A and molecule B in Figure 2 are being pulled apart because the centers of gravity A_c and B_c of the two molecules are located in different planes where

$$dV_x(A\text{–}B) = \dot{\gamma}\, dy \tag{14}$$

and

$$(dy)_{max} = a_g M_A^{1/2} + a_g M_B^{1/2} - 2a_g m_i^{1/2} \tag{15}$$

where $(dy)_{max}$ is the maximum separation of two molecules having an entanglement of shortest segment m_i. Since dy has values from 0 to $(dy)_{max}$, the average is approximately

$$dy = a_g(M^{1/2} - m^{1/2}) \tag{16}$$

The subscript g in eq 15 and 16 indicates that this value of a relates to the radius of gyration of the molecule rather than end-to-end distance.

For random chains, we will use the well-known result

$$a_g^2 = a^2/6.0 \tag{17}$$

As the junction is moving along the chain locus of the disengaging segment at a rate dV_x, the maximum distance it can move is $2aM_e^{1/2}$, as this is the average distance to the next junction, which may be pulling in a different direction at a different rate. The only way we can accomplish disentanglement in this manner is for

$$t_d = \frac{2aM_e^{1/2}}{dV_x} = \frac{aM_e^{1/2}}{\dot{\gamma}a_g(M^{1/2} - m^{1/2})} \tag{18}$$

Substitution of eq 11, 17, and 18 into eq 13 yields

$$V_i = \frac{am_i\dot{\gamma}[1.0 - (m_i/M)]^{1/2}(M^{1/2} - m_i^{1/2})}{6.0^{1/2}M_e} \tag{19}$$

For the monodisperse case, eq 6, 7, 12, and 19 can be directly substituted into eq 5 and integrated for the viscosity

$$\eta_0 = \int_0^{M/2} \frac{4\phi^2\nu[1 - 2m_i/M]}{6.0^{1/2}M}\left(\frac{\xi_0 m_i}{M_0}\right)\left(\frac{am_i}{M_e^{1/2}}\right) \times \left(\frac{am_i}{M_e^{1/2}}\right)\left(1.0 - \frac{m_i}{M}\right)\left[\frac{M^{1/2} - m_i^{1/2}}{M_e^{1/2}}\right] dm_i \tag{20}$$

with the result that

$$\eta_0 = \frac{0.001496\phi^2\nu\xi_0 a^2 M^{3.5}}{M_0(M_e)^{1.5}} \tag{21}$$

Substitution for ν from eq 9 yields for a monodisperse melt

$$\eta_0 = 0.001496(\xi_0/M_0)\rho N(M/M_e)^{2.5}Ma^2 \tag{22}$$

It should be clear that the extra 0.5 power in eq 21 and 22, relative to the tube model predictions, arises because the velocity of the forced reptation in eq 19 is proportional to $M^{0.5}$. Therefore, stresses generated in any linear deformation will be proportional to $M^{3.5}$, although quiescent relaxation of those stresses by tube diffusion will only be proportional to $M^{3.0}$.

It is worthwhile to look at the distribution of relaxation times predicted by this theory for this monodisperse case. The steady-state compliance is defined as

$$J_e^0 = \sum_i \frac{N_i\xi_0^2 L_i^2 P_i^2 V_i^2}{kT\eta_0^2} = \frac{S}{kT\eta_0^2} \tag{23}$$

and the upper summation is given by the integral

$$S = \int_0^{M/2} \frac{4\phi^2\nu[1.0 - 2m_i/M]}{M}\frac{\xi_0 m_i^2}{M_0^2}\frac{a^2 m_i^2}{M_e}\frac{a^2 m_i^2}{6M_e} \times \left(1 - \frac{m_i}{M}\right)^2 \frac{M}{M_e}[1.0 - (m_i/M)^{1/2}]^2\, dm_i \tag{24}$$

$$S = 0.00000551\frac{\phi^2\nu\xi_0^2 a^4 M^7}{M_e^3 M_0^2} \tag{25}$$

$$J_e^0 = \frac{0.00000551}{(0.001496)^2\nu kT\phi^2} = \frac{2.462}{G^0\phi^2} \tag{26}$$

so that for a monodisperse melt, this model predicts

$$J_e^0 G^0 = 2.462 \tag{27}$$

This is right in the range of 1.8–2.8 observed experimentally and is much closer to the observed average than the tube model (1.200) or the Graessley model (1.789).

The crossover between eq 22 and the Rouse expression should occur at the critical molecular weight M_c. The

Rouse expression for velocity in the same nomenclature as eq 22 is

$$(\eta_0)_{\text{Rouse}} = 0.0277\rho N(\xi_0/M_0)Ma^2 \quad (28)$$

Equating eq 22 and 28 at $M = M_c$ yields

$$(M_c/M_e)^{2.5} = 18.52 \quad (29)$$

and therefore

$$M_c = 3.21M_e \quad (30)$$

This agrees quite well with polybutadiene data and that of other polymers with low values of M_e but is somewhat high for polymers with high values of M_e like polystyrene. This distinction between polymers probably relates to random statistics but is beyond the scope of this derivation. In practice, one usually knows M_c/M_e so that the prefactor in eq 22 can be adjusted and a two-constant model can still be obtained.

There is also a crossover between eq 22 and the well-known tube model result.

$$(\eta_0)_{\text{tube}} = 0.10416(\xi_0/M_0)\rho N(M/M_e)^2Ma^2 \quad (31)$$

If we equate eq 22 to eq 31, the crossover molecular weight $M_{FR/D}$ is given by

$$(M/M_e)^{0.5} = 69.9 \quad (32)$$

$$M_{FR/D} = 4848M_e \quad (33)$$

This is higher than any available data. However, the only set of data[16] at high values of M/M_e indicates crossover occurs closer to $500M_e$. These data also indicate that eq 31 yields high results. This may be due to constraint release[12] but a second alternative will be suggested below.

The distinctions between the tube diffusion result and the forced reptation results are better seen if we derive the diffusion result in a network theory format. Let us consider as we did with forced reptation that energy dissipation will be given by eq 4. To obtain the prefactor in eq 31, we need to assume that each entanglement couple is made up of two segments of the same length m_i. The number of junctions of length m_i will then be

$$N_i = 2\phi^2\nu/M \quad (34)$$

The path length will still be given by eq 12 and the segment velocity will be

$$V_i = \frac{am_i\dot{\gamma}[1.0 - (m_i/M)]^{1/2}}{M_e^{1/2}} \quad (35)$$

and as both molecules are allowed to diffuse through the tube defined by their entire length

$$L_i = 2M/M_0 \quad (36)$$

Substitution of eq 12, 34, 35, and 36 into eq 5 yields

$$\eta_0 = \int_0^{M/2} \frac{2\phi^2\nu}{M}\left[\frac{2\xi_0 m_i^2 Ma^2(1.0 - m_i/M)}{M_eM_0}\right] dm_i \quad (37)$$

which yields

$$\eta_0 = \frac{0.10416\phi^2\nu\xi_0M^3a^2}{M_eM_0} \quad (38)$$

which is identical with eq 31. Although the energy dissipation is the same, the distribution of relaxation times is broader due to the focus on junctions. The quantity J_eG^0 is equal to 1.591 for this network formulation.

With the focus on network junctions, two modifications to the tube result seem appropriate. First, junctions would not consist of equal segment size, so that the path length distribution is more appropriately given by eq 7. Second, only the diffusion length of the shortest segment is required to disengage the junction. Then

$$L_i = M/M_0 \quad (39)$$

Substitution of eq 7, 12, 35, and 39 into eq 5 yields

$$\eta_0 = \int_0^{M/2} \frac{4\phi^2\nu(M - 2m_i)}{M^2}\left[\frac{\xi_0 m_i^2 Ma^2(1 - m_i/M)}{M_eM_0}\right] dm_i \quad (40)$$

which yields

$$\eta_0 = \frac{0.02916\phi^2\nu\xi_0M^3a^2}{M_eM_0} \quad (41)$$

The relaxation time distribution of this result is broader still, with $J_eG^0 = 2.055$. At the least, this seems to be the more appropriate result to compare with eq 22. The molecular weight $M_{FR/D}$ at crossover between eq 22 and eq 41 is given by

$$M_{FR/D} = 379.6M_e \quad (42)$$

This result is in good agreement with data[16] that show a gradual crossover from viscosity proportional to $M^{3.41}$ to viscosity proportional to $M^{3.0}$ at ratios of M/M_e between 200 and 2000. On this basis, one could expect the upper limit of application of the forced reptation model to be about $M/M_e = 400$, but this includes just about all commercial polymers.

The formulation of eq 22 and 41 was based on energy dissipation. This was intentional because the result demonstrates that less energy is dissipated by the forced reptation of segments around the entanglement junctions than by coordinated diffusion of the entire molecule along its primitive path. It is reasonable to expect that the mechanism of minimum energy dissipation will be the primary mode of stress relaxation but that the actual behavior will involve elements of both. Figure 3 shows the viscosity data of Colby et al.,[16] Struglinski and Graessley,[5] and Roovers[18] as plotted by Colby et al.,[16] for monodisperse polybutadiene. Quantitative agreement with eq 22 and 41 is excellent. The dash curve in Figure 3 is a combined curve, obtained by adding the reciprocals of the viscosities predicted by the two mechanisms. For about two decades of molecular weight above M_c, the combined model can be adequately represented by $M^{3.4}$. The polybutadiene data also show an increase of about a factor of 10 in η_0/M^3 in the reptation regime, which is consistent with eq 22 and 41. The combined curve could be more accurately calculated by allowing long segments to dissipate energy by tube diffusion and the short segments to dissipate energy by forced reptation. This has not yet been calculated exactly.

In order to use the forced reptation equations directly (ignoring tube diffusion), the best fit to polybutadiene is somewhat below the line shown in Figure 3. For the fit to the monodisperse and blend data of Struglinski and Graessley,[5] we will use from this point on the two constants that are consistent with $M_e = 1733$:

$$G^0 = 1.275 \times 10^7 \text{ dyn/cm}^2 \quad (43)$$

and

$$(\xi_0/M_0)a^2 = 1.71 \times 10^{-25} \text{ (g cm}^2\text{)/s} \quad (44)$$

Using these values, the numerical agreement with the

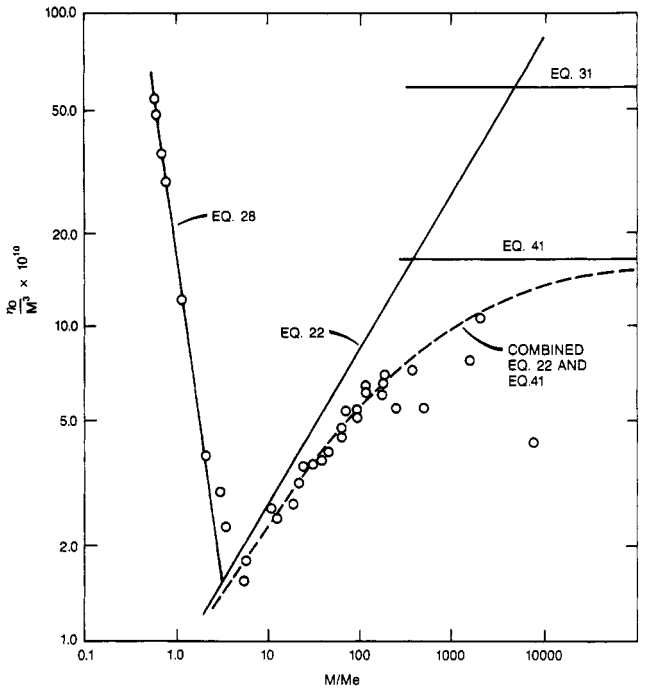

Figure 3. Monodisperse polybutadiene viscosity data at 25 °C[16] plotted as η_0/M^3 versus M/M_e. Solid lines are predictions from Rouse coil motion (eq 28), forced reptation of shortest segment (eq 22), reptation through a tube (eq 31), and modified tube reptation (eq 41).

Table I
Pure-Component Polybutadiene Data at 25 °C[5]

M	η_0(exptl), P	η_0(calcd), P	$10^7 J_e^0$ (exptl), cm²/dyn	$10^7 J_e^0$ (calcd), cm²/dyn
40 700	1.35×10^4	1.49×10^4	1.8	1.93
97 500	3.10×10^5	3.18×10^5	2.0	1.93
174 000	2.95×10^6	2.41×10^6	1.8	1.93
435 000	4.80×10^7	5.97×10^7	2.1	1.93

measured viscosity η_0 and steady-state compliance J_e^0 of the pure-component polybutadienes are shown in Table I.

It is often more convenient to calculate viscoelastic response by using a discrete relaxation function with a set of characteristic times (τ_i) and intensities (G_i) of the relaxation modes. The forced reptation concept introduces motions under deformation that have no counterpart in quiescent relaxation, so that care must be taken when applying the results to all experiments. This paper will confine its attention to stress states developed under shear and to experiments where entanglements pulled apart by forced reptation are small enough in number so that the memory function of the material is unaffected. We can then ignore the distinction and use a set of apparent relaxation times that are not equal to the diffusion times. The apparent relaxation spectra are

$$G_i = kTN_i\Delta m = \frac{4\phi^2 G^0(M - 2m_i)\Delta m}{M^2} \tag{45}$$

and

$$\tau_i = \frac{\xi_0 L_i P_i V_i}{kT} = \frac{\xi_0 a^2 m_i^2 (1.0 - m_i/M)(M^{1/2} - m_i^{1/2})}{6^{1/2} kTM_0 M_e^{1.5}} \tag{46}$$

and

$$m_1 = (M - \Delta m)/2.0 \tag{47}$$

where Δm is the spacing of the discrete spectra.

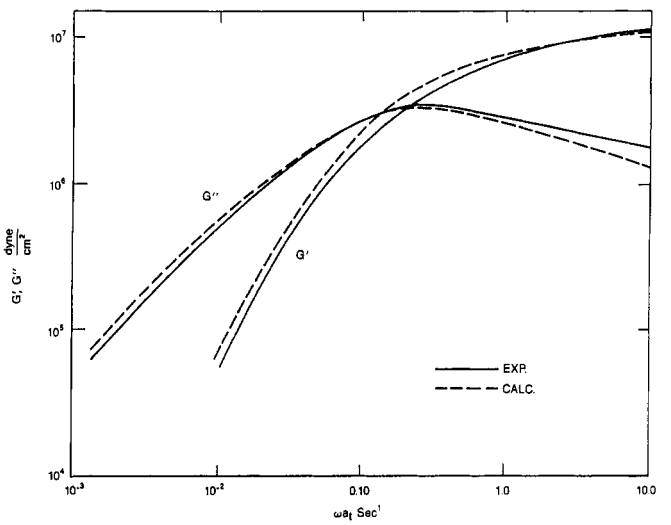

Figure 4. Comparison of forced reptation predictions with storage and loss modulus data for monodisperse polybutadiene data at 25 °C.[5]

For the calculations reported later for polybutadiene, Δm was used as M_e but random statistics do not preclude having segments of noninteger entanglement length multiples. Closer spacing is required to get correct sums when M/M_e is less than 20. By use of eq 45–47, the standard equations can be used for the linear viscoelastic functions.

The zero-shear viscosity η_0 is given by

$$\eta_0 = \sum_i G_i\tau_i \tag{48}$$

The steady-state compliance J_e^0 is given by

$$J_e^0 = \frac{\sum_i G_i\tau_i^2}{(\sum_i G_i\tau_i)^2} \tag{49}$$

The storage modulus G' is given by

$$G' = \sum_i \frac{G_i\omega^2\tau_i^2}{(1.0 + \omega^2\tau_i^2)} \tag{50}$$

and the loss modulus G'' is given by

$$G'' = \sum_i \frac{G_i\omega\tau_i}{(1.0 + \omega^2\tau_i^2)} \tag{51}$$

Figure 4 shows a comparison of the predicted storage and loss modulus using the forced reptation equations for G_i and τ_i and the constants from eq 43 and 44 with the experimental data[5] for polybutadiene of 435 000 molecular weight. Agreement with the shapes of the curves is good over the entire frequency range. The predicted spectra appear to be only slightly narrower than the experimental one.

Extension to Polydisperse Systems

Although eq 22 agrees exceptionally well with data for the monodisperse case, the real power of this approach is displayed by its straightforward extension to polydisperse systems. The first item that is changed is the distribution of shortest segment lengths. Let us consider for now a binary blend of molecules of a long length M_L and a short length M_S. There now are junctions between two molecules of length M_L, two molecules of length M_S, and M_S and M_L. For the M_S–M_L junction, the distribution function is changed because now the maximum value of m_i is

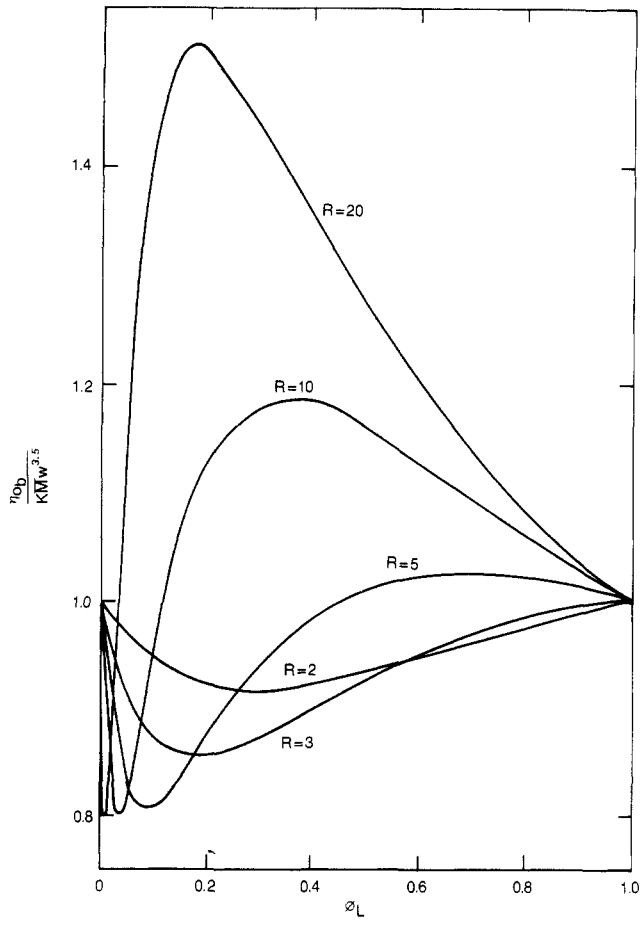

Figure 5. Deviations of the blend viscosity predictions of eq 61 from the empirical rule $\eta_0 \sim \bar{M}_w^{3.5}$ as a function of volume fraction of the high molecular weight component ϕ_L and the molecular weight ratio R.

$M_S/2$. The distribution of shortest segments is

$$N_i = \frac{4\phi_L\phi_S\nu[M_L + M_S - 4m_i]}{M_L M_S} \tag{52}$$

as required by a distribution function

$$\int_0^{M_S/2} N_i \, dm_i = 2\phi_L\phi_S\nu \tag{53}$$

which is the density of junctions between M_L and M_S.

The average value of the shortest segment length m is given by

$$\bar{M} = \int_0^{M_S/2} \frac{N_i m_i \, dm_i}{2\phi_L\phi_S\nu} = \frac{M_S}{4}\left[1.0 - \frac{M_S}{3M_L}\right] \tag{54}$$

Note that $\bar{M}$ increases from $M_S/6.0$ in a junction between two short chains to $M_S/4.0$ in a junction between a short chain and a very long chain.

The second modification that needs to be made for blends is in the path term. The path of a segment m depends on the composition of the matrix. If we continue to assume that junctions are distributed according to the volume fractions of the components, then

$$P_i = \phi_L P_i(m_i/M_L) + \phi_S P_i(m_i/M_S) \tag{55}$$

and as m_i is always less than $M_S/2$

$$P_i = \phi_L(1.0 - m_i/M_L) + \phi_S(1.0 - m_i/M_S) \tag{56}$$

Equation 56 also holds for the junctions between two short molecules and some of the junctions between two long molecules. However, some of the junctions between long molecules have a shortest segment that is greater than $M_S/2$. In this case

$$P_i = \phi_L(1.0 - m_i/M_L) + \phi_S(0.25M_S/m_i) \tag{57}$$

The velocity term is simply adjusted for the blend case as the analogous equation to eq 15 for the mixed entanglement is

$$(dy)_{max} = a_g M_L^{1/2} + a_g M_S^{1/2} - 2a_g m_i^{1/2} \tag{58}$$

Equations 52, 56, 57, and 58 can be substituted into eq 5 and integrated to solve for the viscosity of the blend. To simplify matters, the common terms are lumped and labeled B.

$$B = 4\nu\xi_0 a^2/M_0 M_e^{3/2} \tag{59}$$

Then

$$\eta_0 = \int_0^{M_S/2} B\phi_L^2 \frac{[M_L - 2m_i]}{M_L^2} m_i^3 \left[\phi_L\left(1.0 - \frac{m_i}{M_L}\right) + \phi_S\left(1.0 - \frac{m_i}{M_S}\right)\right][2M_L^{1/2} - 2m_i^{1/2}] \, dm_i +$$
$$\int_{M_S/2}^{M_L/2} B\phi_L^2 \frac{[M_L - 2m_i]}{M_L^2} m_i^3 \left[\phi_L\left(1.0 - \frac{m_i}{M_L}\right) + \phi_S\left(0.25\frac{M_S}{m_i}\right)\right][2M_L^{1/2} - 2m_i^{1/2}] \, dm_i +$$
$$\int_0^{M_S/2} B\phi_L\phi_S \frac{[M_L + M_S - 4m_i]}{M_L M_S} m_i^3 \left[\phi_L\left(1.0 - \frac{m_i}{M_L}\right) + \phi_S\left(1.0 - \frac{m_i}{M_S}\right)\right][M_L^{1/2} + M_S^{1/2} - 2m_i^{1/2}] \, dm_i +$$
$$\int_0^{M_S/2} B\phi_S^2 \frac{[M_S - 2m_i]}{M_S^2} m_i^3 \left[\phi_L\left(1.0 - \frac{m_i}{M_i}\right) + \phi_S\left(1.0 - \frac{m_i}{M_S}\right)\right][2M_S^{1/2} - 2m_i^{1/2}] \, dm_i \tag{60}$$

where the first two integrals describe energy dissipation related to $M_L - M_L$ entanglements, the third integral relates to $M_S - M_L$ entanglements, and the fourth integral relates to $M_S - M_S$ entanglements.

Equation 60 can be integrated and rearranged to yield a blending rule for viscosity

$$\eta_{0b} = \eta_{0L}\phi_L^3\left[1.0 + 1.312\frac{M_S}{M_L}\frac{\phi_S}{\phi_L}\right] + \eta_{0S}\phi_S^3\left\{1.0 + 5.116\frac{\phi_L}{\phi_S}\left[(M_L/M_S)^{1/2} + 0.0477 - 0.555(M_S/M_L)^{1/2} + 0.094\frac{M_S}{M_L}\right] + 7.480\frac{\phi_L^2}{\phi_S^2}\left[(M_L/M_S)^{1/2} - 0.238 - 1.023(M_S/M_L)^{1/2} + 0.335\frac{M_S}{M_L} + 0.251(M_S/M_L)^{3/2} - 0.0983(M_S/M_L)^2\right]\right\} \tag{61}$$

The form of this equation is interesting because it does not resemble at all a weight-average blending law. How-

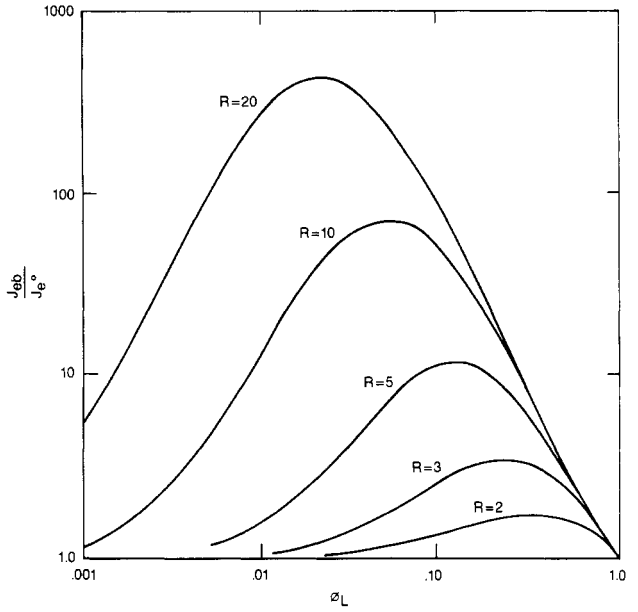

Figure 6. Predictions of the reduced steady-state compliance (J_{ep}/J_e^0) as a function of blend composition ϕ_L and the molecular weight ratio R using eq 45, 46, 47, and 49.

ever, the predictions are much closer than is apparent from the form. The predictions of eq 61 are shown in Figure 5. Below ratios of M_L/M_S of 3.0, the predicted viscosity of the blend is somewhat below the weight-average blending rule for all mixtures. However, the difference is never greater than 15%. For mixtures with M_L/M_S greater than 10.0, the predicted viscosity is greater than the weight-average blending rule over most of the composition range, with a maximum deviation that increases and occurs at lower weight fractions as the ratio M_L/M_S is increased. Comparison with data will be left to the following section.

Predictions of the steady-state compliance of blends are also obtainable from the forced reptation theory. Using the blending equations derived in this section and eq 23, the integrations can be performed to give a numerical blending equation for compliance similar to eq 61 for viscosity. The form of this equation is not particularly instructive, however, so that calculations of the compliance and the storage and loss modulus have all been done by using summations of the relaxation spectra. The predicted curves of the steady-state compliance of binary blends of M_L and M_S are shown in Figure 6. This is plotted on a log–log plot to better show the shapes of the curves. The predicted curves are given as ratios to the pure component so that they are independent of the entanglement molecular weight and the monomeric friction of the material. The same curves apply to all polymers as long as the relaxations of less than one entanglement length can be ignored and diffusion through the tube can be ignored. As long as both components have a reduced molecular weight (M/M_e) greater than 5 but less than 500, this should be reasonable. The reduced viscosity curves and compliance curves for blends are independent of the constants characteristic of the material, G^0 and ξ^0, as long as all components are in the entangled region. The shapes of these curves are similar to many that have been published in the literature. Quantitative comparison to data will be left to the next section.

Comparison of Binary Blend Predictions to Data

Using the equations developed for blends and the two constants obtained from pure-component data, all linear viscoelastic behavior of blends can be predicted. The Struglinski–Graessley data for binary butadiene blends are

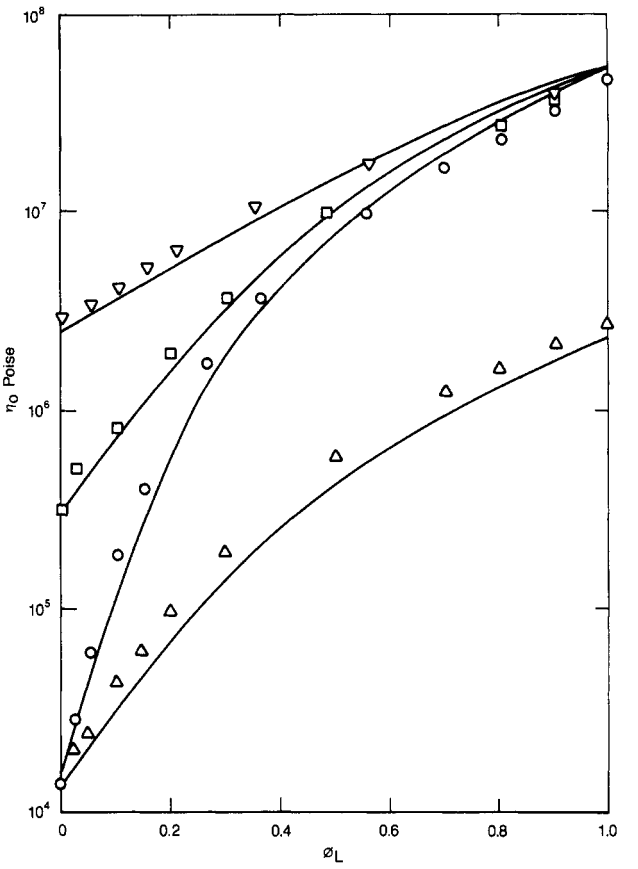

Figure 7. Prediction of the viscosities of binary polybutadiene blends at 25 °C[5] using eq 61 and the constants from eq 43 and 44. The points are data from ref 5 for blends 435/41 (○), 435/98 (□), 435/174 (▽), and 174/41 (△), and solid lines are predictions.

focused on here, because all components of their blends are well into the entangled regime. Figure 7 shows a comparison of the viscosity predictions of eq 60 with the experimental data. Agreement is excellent with the shapes of the curves of all four of these blends. Most of the discrepancies are due to the end points because $\eta_0 \propto M^{3.4}$ rather than $\eta_0 \propto M^{3.5}$ for the forced reptation theory. The deviations of the Struglinski–Graessley data from the weight-average blending rule are shown in Figure 8. These were generated by fitting the end points to $\eta_0 = (\bar{M}_w)^x$ and calculating the ratios of $(\eta_0)_{exp}/(\bar{M}_w)^x$. This adjusts for deviations of the pure component from exact agreement with the $M^{3.41}$ rule. The reason for this exercise is to show that the shapes of the curves obtained are similar to those calculated from the theory in Figure 5. At low ratios of M_L/M_S, the blends show small negative deviations from the weight-average rule, and at ratios of 4.5 and above, they show positive deviations, with increasing deviation at higher ratios. The location of the experimental maximum deviation is similar in volume fraction to the calculated one (0.28 and 0.32).

Figure 9 shows the calculated values for steady-state compliance, using the same two constants compared to the data of Struglinski and Graessley. The shapes of the curves show generally excellent agreement. However, the predicted magnitude of the compliance peak is low for both the R = 2.5 and R = 4.5 ratios and only shows good agreement at R = 10.7. It is not clear why this occurs when the predicted blend viscosities are so uniformly good.

Figures 10 and 11 show the loss modulus data for polybutadiene blends with the loss modulus on a linear scale as plotted in ref 5. This method of plotting hides the behavior in the long-time end of the spectrum but shows more detail of the shape of the loss peaks. The forced

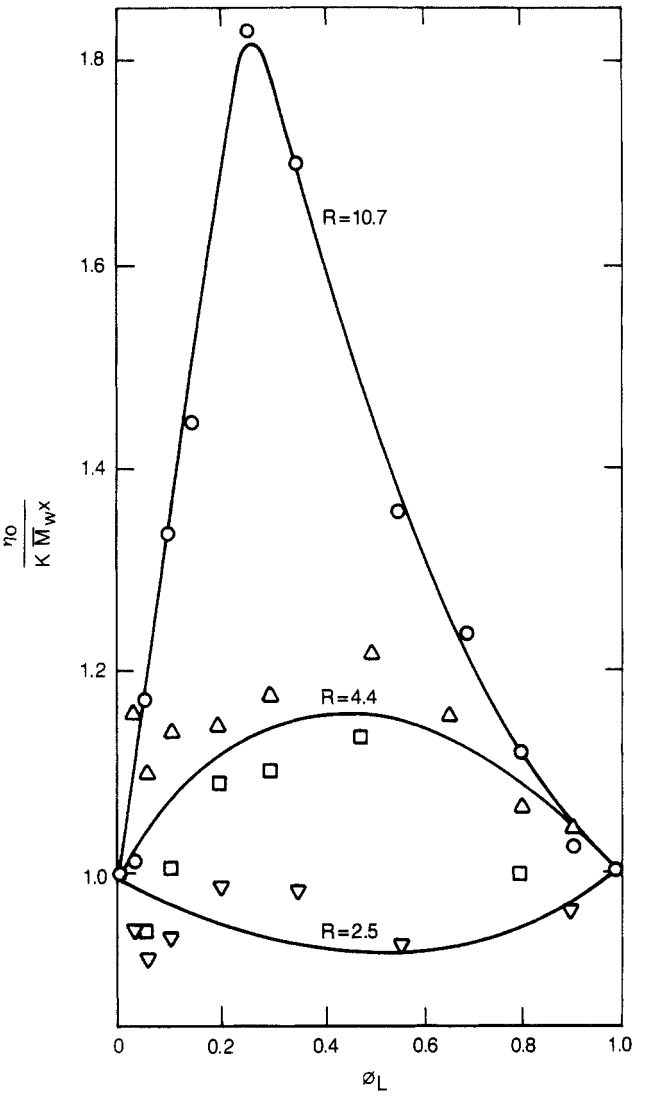

Figure 8. Deviations of the blend viscosity data of ref 5 from empirical rule $\eta_0 \sim \bar{M}_w^x$ where x is defined by pure-component data. Solid lines are drawn through points for comparison to Figure 5.

reptation predictions using the constants from eq 43 and 44 are shown as the solid lines in Figures 10 and 11. The shifts in the frequency and magnitude of the loss peaks of the high and low molecular weight components are fairly well predicted. The only significant discrepancy between the predicted and experimental curves seem to be some extra relaxations in the predicted curves in the intermediate frequency range between the two peaks. Errors in this region are generally less than 20% but seem to be greater than experimental errors.

Discussion of Results

In addition to the quantitative description of the polybutadiene blend response, it is of interest to look at some of the limiting cases of behavior that are more easily measurable in polystyrene blends. It has consistently been observed that the viscosity of dilute solutions of a high molecular weight polystyrene in a low molecular weight polystyrene can be described by

$$(\eta_{0b} - \phi_s \eta_{0S}) \propto \phi_L \tag{62}$$

It can easily be shown from eq 61 that for the dilute case when $M_L \gg M_S$

$$(\eta_{0b} - \phi_S^3 \eta_{0S}) = 5.116 \phi_S^2 \phi_L \eta_{0S} (M_L/M_S)^{1/2} \tag{63}$$

This appears to match the dependence on ϕ_L, η_{0S}, M_L, and

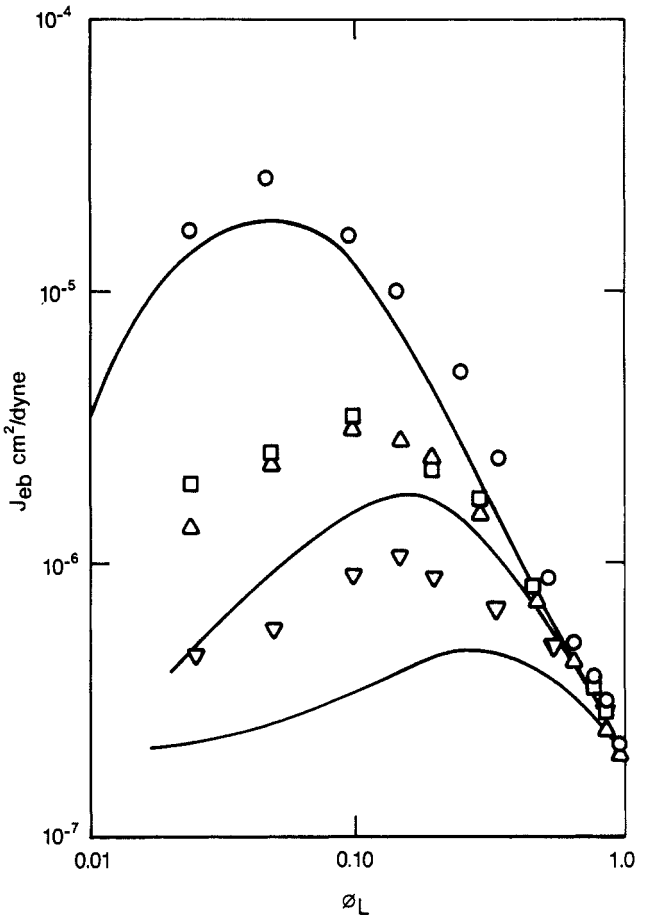

Figure 9. Prediction of the steady-state compliance of binary polybutadiene blends at 25 °C from ref 5 using eq 45, 46, 47, and 49 and the constants from eq 43 and 44. The points are data for blends 435/41 (○), 435/98 (□), 435/174 (▽), and 174/41 (△), and solid lines are predictions.

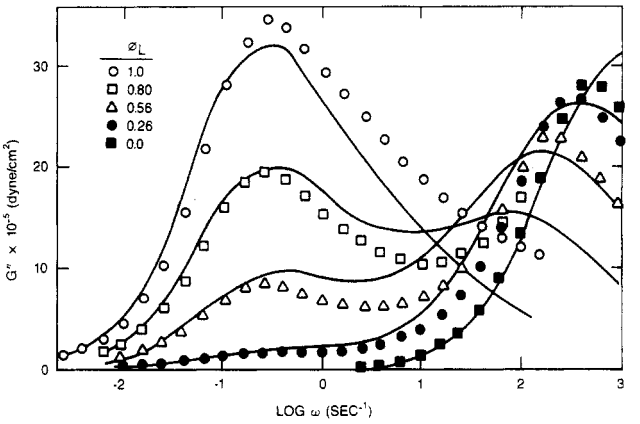

Figure 10. Comparison of predictions of the forced reptation model for the loss modulus of binary polybutadiene blends 435/41 at 25 °C to the data from ref 5.

M_S seen by Watanabe and Kotaka[19] for dilute solutions of a high molecular weight polystyrene in a low molecular weight polystyrene with $M_S > M_e$. The measured constant in eq 63 appears to be closer to 10 than 5. However, because the parametric dependence is right and the $(M_L/M_S)^{1/2}$ term comes from the velocity term in the forced reptation mechanism, this is further evidence that the phenomenological description corresponds to reality.

The second limiting case of interest is concentrated solutions. It has often been cited[5,20] that there is a distinction between polybutadiene blends where $M_L M_e^2/M_S^3 \ll 1.0$ and many polystyrene blends where $M_L M_e^2/M_S^3 >$

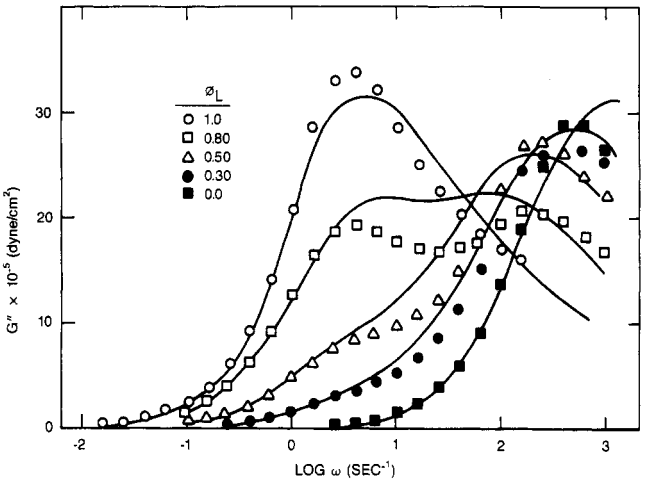

Figure 11. Comparison of predictions of forced reptation model for the loss modulus of binary polybutadiene blends 174/41 at 25 °C to the data from ref 5.

1.0. The present theory predicts no distinction between these cases for concentrated solutions of M_L as long as $M_S/M_e > 6$. For the case where $M_S/M_e > 6$ and $M_L/M_S > 10$, the theory suggests that

$$\tau_{LL} \propto \phi_L M_L^{3.5} \tag{64}$$

Watanabe and Kotaka[19] found for polystyrene blends that

$$\tau_{LL} \propto \phi_L^{(1.0-1.5)} M_L^{3.5} \tag{65}$$

where values of the exponent decreased from 1.5 for $M_s/M_e < 2$ to 1.0 for $M_s/M_e = 3.7$. Certainly we would expect that blends with a short component less than $2M_e$ would act more like dilution with a solvent. For the solvent case, eq 21 predicts that

$$\eta_0 \propto \phi^{3.5} M^{3.5} \tag{66}$$

$$G^0 \propto \phi^2 \tag{67}$$

$$\tau \propto \phi^{1.5} M^{3.5} \tag{68}$$

which is in agreement with the data quoted above for dilution with low molecular weight chains and in agreement with most data for concentrated solutions in a solvent.

The forced reptation equations have been developed by using a steady-shear field. This was chosen to elucidate the physical mechanism of molecular motion in response to a shear field. It should be clear, however, that to generalize this concept to a constitutive equation requires some new developments because the appropriate strain tensor on a micro scale is molecular weight dependent. Careful comparison of response during strain to response in a static test may help prove or disprove the forced reptation concept.

Summary

The forced reptation model that phenomenologically describes reptation of the shortest segment of an entanglement coupled around the entanglement junction shows both qualitative and quantitative agreement with experimental data on entangled linear polymers. Although this model is similar in concept to the Graessley model,[2] it is distinguished from this model by using a molecular network approach to define the junction length distribution and by using reptation with constraint release to define the paths and rates of segment motion. This is a two-constant model and both constants given by eq 43 and 44 agree well with generally accepted values. The vast superiority of this model to any other two-constant model is taken as evidence that the molecular dynamics described is the primary mode of motion over most of the entangled region.

The model suffers from the same difficulty as other reptation models in that the primary path length is difficult to define quantitatively, although good agreement is obtained with polybutadiene data using the root-mean-square end-to-end distance of the molecular weight between entanglements as the characteristic length. For polymers where the ratio M_c/M_e is not equal to 3.2, one can use M_e to determine G^0 and M_c to define the friction term in the entangled region and then use these values to predict all linear viscoelastic behavior of the polymer and its blends.

It should be reasonably clear that this description of polymer molecule dynamics in a deformation field is superposed on the Brownian motion of chains, which occurs whether or not the material is being deformed. The molecular diffusion follows the well-known M^{-2} dependence predicted by reptation theory even when in the region where $\eta_0 \sim M^{3.4}$. An interplay between the velocity field imposed dynamics and the Brownian motion only occurs in the nonlinear viscoelastic region when entanglements are being pulled apart by forced reptation faster than they are formed by diffusion. This will be the subject of a subsequent paper.

Acknowledgment. Special thanks to W. W. Graessley whose many papers in the field have influenced the author's thought process. Thanks also to The Dow Chemical Co. for allowing publication of this work.

Registry No. Polybutadiene, 9003-17-2.

References and Notes

(1) Graessley, W. W. *J. Chem. Phys.* **1967**, *47*, 1942.
(2) Graessley, W. W. *J. Chem. Phys.* **1971**, *54*, 5143.
(3) Graessley, W. W. *Adv. Polym. Sci.* **1974**, *16*, 1.
(4) Bernard, D. A.; Noolandi, J. *Macromolecules* **1982**, *15*, 1553.
(5) Struglinski, M. J.; Graessley, W. W. *Macromolecules* **1985**, *18*, 2630.
(6) Watanabe, H.; Sakamoto, T.; Kotaka, T. *Macromolecules* **1985**, *18*, 1008.
(7) Prest, W. M. *J. Polym. Sci., A-2* **1970**, *8*, 1897.
(8) de Gennes, P.-G. *J. Chem. Phys.* **1971**, *55*, 572.
(9) Doi, M.; Edwards, S. F. *The Theory of Polymer Dynamics*, Clarendon Press: Oxford, 1986.
(10) Green, P. F.; Kramer, E. J. *Macromolecules* **1986**, *19*, 1108.
(11) Marrucci, G. *J. Polym. Sci., Polym. Phys. Ed.* **1985**, *23*, 159.
(12) Graessley, W. W.; Struglinski, M. J. *Macromolecules* **1986**, *19*, 1754.
(13) Montfort, J. P.; Marin, G.; Monge, P. *Macromolecules* **1984**, *17*, 1551.
(14) Rubinstein, M.; Helfand, E.; Pearson, D. *Macromolecules* **1987**, *20*, 822.
(15) Doi, M. J. *Polym. Sci., Polym. Lett. Ed.* **1981**, *19*, 265.
(16) Colby, R. H.; Fetters, L. J.; Graessley, W. W. *Macromolecules* **1987**, *20*, 2226.
(17) Pearson, D. J. *Rubber Chem. Technol.* **1987**, *60*, 439.
(18) Roovers, J. *Polym. J.* **1986**, *18*, 153.
(19) Watanabe, H.; Kotaka, T. *Macromolecules* **1984**, *17*, 2316.
(20) Daoud, M.; de Gennes, P.-G. *J. Polym. Sci., Polym. Phys. Ed.*, **1979**, *17*, 1971.